Sliding-Mode MRAS Speed Estimator for Sensorless Vector Control of Double Stator Induction Motor

Houari Khouidmi[1*], Ahmed Benzouaoui[2], Boubaker Bessedik[2]
1- Hassiba Benbouali University of Chlef. Po.Box 151 Hay Es-Salem Chlef 02000-Algeria.
Email: h.khouidmi@univ-chlef.dz (Corresponding author)
2- University of Sciences and Technology USTO-MB of Oran. P.O. Box 1505, El M`nouar, Oran 31000-Algeria.
Email: a.benzouaoui@univ-usto.dz, b.bessedik@univ-usto.dz

Received: November 2017 Revised: February 2018 Accepted: March 2018

ABSTRACT:
The weakness of the Direct Vector Control (DVC) is lack of an estimation of the flux amplitude and the rotor position with high accuracy. These quantities are sensitive to parameter variations; it is important to use a robust estimation system for estimating the rotor flux with respect to parametric uncertainties. In this paper the sliding mode speed sensorless vector control based on the Model Reference Adaptive System (MRAS) of double stator induction motor is presented. First, the models of the double stator induction motor and the DVC are proposed. Second, the MRAS technique of the DSIM is adopted. In order to ensure a robust sensorless control, the sliding mode technique for the estimation system was used. The results showed the presented estimator has a positive effect on the system behavior especially in changing the reference and/or the parameters variation.

KEYWORDS: Double Stator Induction Motor, Direct Field Oriented Control, Model Reference Adaptive System, Sliding Mode Control, Sensorless Control.

1. INTRODUCTION

In the areas of "control of electrical machines", the research works are oriented increasingly to sensorless control techniques [1-3], where the performance of control laws depend on the degree of precision in the knowledge of the flux amplitude and its position. These quantities are easily accessible by steps. Indeed, flux sensors are relatively difficult (measurement noise) and reduce the strength of the whole. Thus, the reconstruction of flux or its position estimators or observers becomes a primary goal [4-6]. In this context, the sliding mode estimation strategy based on model reference adaptive system MRAS has been used [7], [8].

The Field Oriented Control (FOC), developed for Double Stator Induction Machine (DSIM), requires the measurement of the speed to perform the coordinate transformations. Physically, this measurement is performed using a mechanical speed sensor mounted on the rotor shaft, which unfortunately increases the complexity and cost of installation (additional wiring and maintenance) [3-5]. Moreover, the mechanical speed sensors are usually expensive, fragile and affect the reliability of the control. In this context, our study focuses mainly on the speed estimation using the model reference adaptive system observer for a sensorless vector control of a double stator induction motor.

The speed estimator based on the theory of model reference adaptive system is the most popular techniques that have been implemented for the sensorless speed controlling of induction motor using only the measurements of stator voltage and current [8,9]. This approach is based on a reference model of the machine (usually it is a voltage model) does not depend on the rotor speed, and an adjustable model (usually it is a current model) directly dependent on the speed. The error between the two models injected in an adaptation mechanism.

The Sliding Mode (SM) is a particular operation mode of variable structure systems. The theory of these systems has been studied and developed in the Soviet Union, first by Professor Emelyanov [10], then by other collaborators like Utkin, from the study's results of the mathematician Filippov on the discontinuous second-member differential equations. Then the works were resumed in the United States by Slotine [11] in Japan by Young, Harashima and Hashimoto.

The main contribution of this paper is the implementation of a high-performance sliding mode sensorless control scheme for a double stator induction motor, this control strategy is used to estimate the speed and the rotor flux to generate the switching states of the inverter and consequently the supply voltages of the DSIM.

The paper is organized as follows: the DSIM model and the vector control strategy are presented in section 2 and 3 respectively. In Section 4 the Model Reference Adaptive System (MRAS) strategies are discussed. Section 5 is devoted to the sliding-mode technique, section 6 provides the application of the resulting sensorless control. Finally, the overall proposed sliding-mode MRAS estimator for speed sensorless control of DSIM shown in Fig.1 is used for numerical simulation and the related results and remarks are presented.

2. DSIM MODEL

The equations of the double stator induction machine can be expressed in (α, β) axes where the attributed reference is the stator field [12], [13].

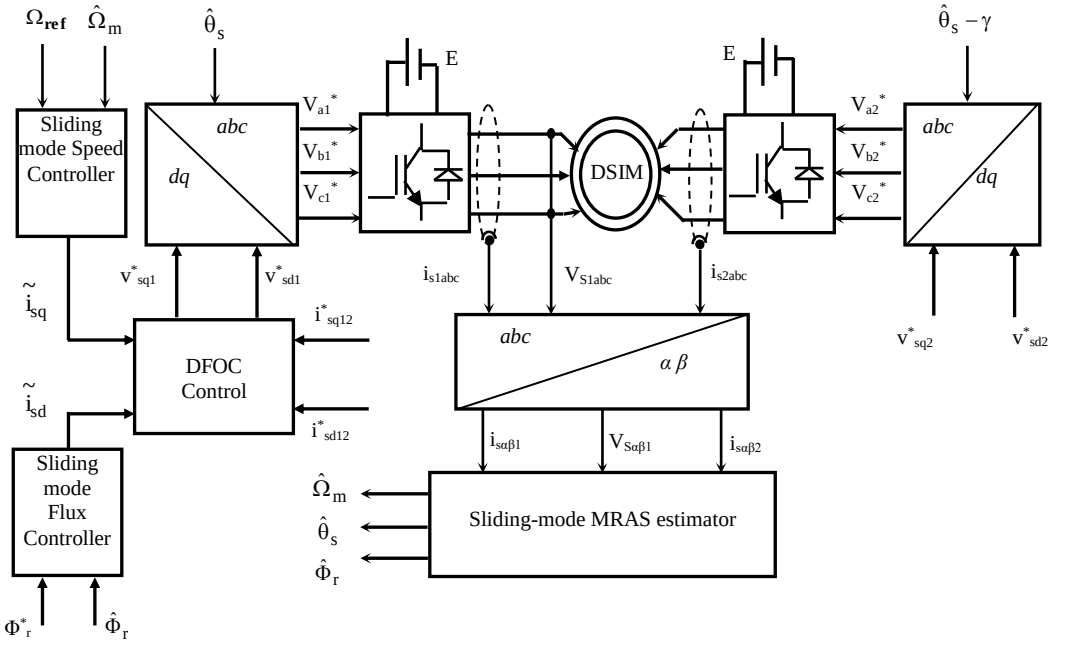

Fig.1. Sliding mode sensorless vector control scheme of DSIM.

Voltages Equations

By choosing a referential related to the stator field, we obtain the following system of equations [12-14]:

$$\begin{cases} v_{s\alpha1} = R_{s1} i_{s\alpha1} + \dfrac{d\Phi_{s\alpha1}}{dt} \\ v_{s\beta1} = R_{s1} i_{sq1} + \dfrac{d\Phi_{s\beta1}}{dt} \\ v_{s\alpha2} = R_{s2} i_{s\alpha2} + \dfrac{d\Phi_{s\alpha2}}{dt} \\ v_{s\beta2} = R_{s2} i_{s\beta2} + \dfrac{d\Phi_{s\beta2}}{dt} \\ 0 = R_r i_{r\alpha} + \dfrac{d\Phi_{r\alpha}}{dt} + \omega_m \Phi_{r\beta} \\ 0 = R_r i_{r\beta} + \dfrac{d\Phi_{r\beta}}{dt} - \omega_m \Phi_{r\alpha} \end{cases} \quad (1)$$

Where:

$v_{s1\alpha\beta}$ $v_{s2\alpha\beta}$:First and second stator voltages in stationary frame

$i_{s1\alpha\beta}$ $i_{s2\alpha\beta}$:First and second stator currents in stationary frame

$\Phi_{s1\alpha\beta}$ $\Phi_{s2\alpha\beta}$:First and second stator flux in stationary frame

$\Phi_{r\alpha\beta}$:Rotor flux in stationary frame

ω_m :Rotor angular frequency

R_{s12} R_r :First and second stator and rotor resistance

Flux Equations

The relations between flux and currents are given by [12-14]:

$$\begin{cases} \Phi_{s\alpha1} = L_{s1} i_{s\alpha1} + L_m (i_{s\alpha1} + i_{s\alpha2} + i_{r\alpha}) \\ \Phi_{s\beta1} = L_{s1} i_{s\beta1} + L_m (i_{s\beta1} + i_{s\beta2} + i_{r\beta}) \\ \Phi_{s\alpha2} = L_{s2} i_{s\alpha2} + L_m (i_{s\alpha1} + i_{s\alpha2} + i_{r\alpha}) \\ \Phi_{s\beta2} = L_{s2} i_{s\beta2} + L_m (i_{s\beta1} + i_{s\beta2} + i_{r\beta}) \\ \Phi_{r\alpha} = L_r i_{r\alpha} + L_m (i_{s\alpha1} + i_{s\alpha2} + i_{r\alpha}) \\ \Phi_{r\beta} = L_r i_{r\beta} + L_m (i_{s\beta1} + i_{s\beta2} + i_{r\beta}) \end{cases} \quad (2)$$

Where:
L_{s12} :First and second stator inductance
L_r :Rotor inductance
L_m :Mutual inductance
Replacing the system of equations (2) in (1) we obtain the mathematical DSIM model (3).

$$\begin{cases} v_{s\beta2} = R_{s2} i_{s\beta2} + (L_{s2} + L_m)\sigma \dfrac{di_{s\beta2}}{dt} + \\ \quad + \dfrac{L_m L_r}{L_m + L_r} \dfrac{di_{s\beta1}}{dt} + \dfrac{L_m}{L_m + L_r} \dfrac{d\Phi_{r\beta}}{dt} \\ 0 = -\dfrac{L_m}{T_r}(i_{s\alpha1} + i_{s\alpha2}) + \dfrac{1}{T_r}\Phi_{r\alpha} + \\ \qquad + \dfrac{d\Phi_{r\alpha}}{dt} + \omega_m \Phi_{r\beta} \\ 0 = -\dfrac{L_m}{T_r}(i_{s\beta1} + i_{s\beta2}) + \dfrac{1}{T_r}\Phi_{r\beta} + \\ \qquad + \dfrac{d\Phi_{r\beta}}{dt} - \omega_m \Phi_{r\alpha} \end{cases}$$

$$\begin{cases} v_{s\alpha1} = R_{s1} i_{s\alpha1} + (L_{s1} + L_m)\sigma \dfrac{di_{s\alpha1}}{dt} + \\ \quad + \dfrac{L_m L_r}{L_m + L_r} \dfrac{di_{s\alpha2}}{dt} + \dfrac{L_m}{L_m + L_r} \dfrac{d\Phi_{r\alpha}}{dt} \\ v_{s\beta1} = R_{s1} i_{s\beta1} + (L_{s1} + L_m)\sigma \dfrac{di_{s\beta1}}{dt} + \\ \quad + \dfrac{L_m L_r}{L_m + L_r} \dfrac{di_{s\beta2}}{dt} + \dfrac{L_m}{L_m + L_r} \dfrac{d\Phi_{r\beta}}{dt} \\ v_{s\alpha2} = R_{s2} i_{s\alpha2} + (L_{s2} + L_m)\sigma \dfrac{di_{s\alpha2}}{dt} + \\ \quad + \dfrac{L_m L_r}{L_m + L_r} \dfrac{di_{s\alpha1}}{dt} + \dfrac{L_m}{L_m + L_r} \dfrac{d\Phi_{r\alpha}}{dt} \end{cases} \quad (3)$$

With:

$$\sigma = 1 - \frac{L_m^2}{(L_m + L_r)(L_m + L_s)},$$

$$L_{s1} = L_{s2} = L_s,$$

$$T_r = \frac{L_m + L_r}{R_r}$$

Where:
σ :Total leakage factor;
T_r :Rotor time constant.

Mechanical Equations
The equation of the electromagnetic torque is [14]:

$$T_{em} = p\frac{L_m}{L_m + L_r}\left[(i_{s\beta1} + i_{s\beta2})\Phi_{r\alpha} - (i_{s\alpha1} + i_{s\alpha2})\Phi_{r\beta}\right] \quad (4)$$

Where:
T_{em} : Electromagnetic torque;
p :Number of pole pairs

The mechanical equation is:

$$J\frac{d\Omega_r}{dt} = T_{em} - T_L - k_f \Omega_m \quad (5)$$

Where:
J :Inertia;
Ω_m :Mechanical rotor speed
T_L :Load torque
k_f :Viscous friction coefficient

3. DIRECT FIELD ORIENTED CONTROL OF DSIM

In the direct vector control, knowledge of the rotor flux (amplitude and phase) is required to ensure the decoupling between the torque and flux. Indeed, the position of the rotor flux θ_s is calculated algebraically from the information on the rotor flux [5], [6].

$$\begin{cases} \hat{\Phi}_r = \sqrt{\Phi_{r\alpha}^2 + \Phi_{r\beta}^2} \\ \hat{\theta}_s = \text{arctg}\left(\dfrac{\Phi_{r\beta}}{\Phi_{r\alpha}}\right) \end{cases} \quad (6)$$

These components can beings expressed from the DSIM voltage model; equation (3):

$$\begin{cases} \Phi_{r\alpha} = \dfrac{L_r + L_m}{L_m}\displaystyle\int \left[V_{s\alpha1} - R_s i_{s\alpha1} - \sigma(L_s + L_m)\frac{di_{s\alpha1}}{dt} - \right. \\ \qquad \left. - \dfrac{L_m L_r}{L_m + L_r}\dfrac{di_{s\alpha2}}{dt} \right] dt \\ \Phi_{r\beta} = \dfrac{L_r + L_m}{L_m}\displaystyle\int \left[V_{s\beta1} - R_s i_{s\beta1} - \sigma(L_s + L_m)\frac{di_{s\beta1}}{dt} - \right. \\ \qquad \left. - \dfrac{L_m L_r}{L_m + L_r}\dfrac{di_{s\beta2}}{dt} \right] dt \end{cases} \quad (7)$$

The principle of orientation shown in Figure 4 aligns the rotor flux on the direct axis of Park's axes [4], [13].

Thus, we obtain for the orientation of the rotor flux:

$$\begin{cases} \Phi_r = \Phi_{rd} \\ \Phi_{rq} = 0 \end{cases} \quad (8)$$

The following equations of rotor flux and electromagnetic torque are used:

$$\begin{cases} \dfrac{d\Phi^*_r}{dt} = \dfrac{1}{T_r}\left[L_m(i^*_{sd1} + i^*_{sd2}) - \Phi^*_r\right] \\ T^*_{em} = p\dfrac{L_m}{L_m + L_r}\left[(i^*_{sq1} + i^*_{sq2})\Phi^*_r\right] \end{cases} \quad (9)$$

After Laplace transform, we can write:

$$\begin{cases} \Phi^*_r = \dfrac{L_m}{1 + T_r s}(i^*_{sd1} + i^*_{sd2}) \\ T^*_{em} = p\dfrac{L_m}{L_m + L_r}\left[(i^*_{sq1} + i^*_{sq2})\Phi^*_r\right] \end{cases} \quad (10)$$

The two stator's windings are identical, so the powers provided by this two windings system are the same, hence:

$$\begin{cases} i^*_{sd1} = i^*_{sd2} = \dfrac{1 + T_r s}{2L_m}\Phi^*_r \\ i^*_{sq1} = i^*_{sq2} = p\dfrac{L_m + L_r}{2L_m\Phi^*_r}T^*_{em} \end{cases} \quad (11)$$

4. CONCEPTS OF ESTIMATORS

Estimators used in open loop, based on the use of the model of the controlled system [4-6, 8]. The dynamics of an estimator depends on the specific modes of the system. Such an approach leads to the implementation of simple and fast algorithms, but sensitive to modeling errors and parametric variations or during operation. Indeed, there is no closure with real variables to consider these errors or disturbances. Such an estimator is shown in Figure 2.

The system shown in Figure 2 is defined by the state form as follows [4]:

$$\begin{cases} \dfrac{dX}{dt} = A(\Omega)X + BU \\ Y = CX \end{cases} \quad (12)$$

Where *B* is the input matrix of the system, *C* is the output matrix and *A(Ω)* is the non-stationary transition matrix of our system, since it depends on the rotational speed. However, it can be considered as quasi-stationary for the dynamics speed with respect to that of the electrical quantities.

By integrating equation (12), we can reconstruct the estimate state.

$$\hat{X} = \int\left(\hat{A}(\Omega)\hat{X} + \hat{B}.U\right)dt \quad (13)$$

To evaluate the accuracy of the estimate, we consider the difference between the measured and estimated states:

$$\varepsilon = X - \hat{X} \quad (14)$$

Then the dynamic error is deduced from relations (12) and (13):

$$\frac{d\varepsilon}{dt} = A(\Omega)\varepsilon + \Delta A\hat{X} + \Delta BU \quad (15)$$

Where:

$\Delta A = A(\Omega) - \hat{A}(\Omega)$ and $\Delta B = B - \hat{B}$

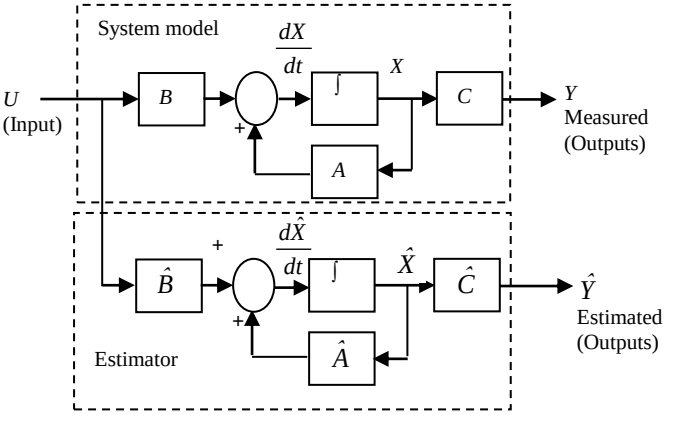

Fig.2. The structure of an estimator.

The convergence speed of the estimation error depends on the time constants of the system. It is checked in case the eigenvalues of the state matrix are defined negative (considering $\Delta A = 0$ and $\Delta B = 0$). When modeling errors exist, the terms *ΔAX* and *ΔBU* behave as inputs in equation (15). In the case of electrical machines, we do not control the convergence time of the estimation error, and the estimates have necessarily a static error due to modeling errors [4].

5. MODEL REFERENCE ADAPTIVE SYSTEM

The approach by the model reference adaptive system MRAS was proposed by Shauder [16] thereafter, it has been exploited by several studies [7-9].

As its name suggests MRAS, it is based on identification between adaptive and reference model to estimate the speed. In its simplest form, the MRAS structure as shown in Figure 3 consists of two estimators that calculate the same variables of the system, the first is a reference model that represents the machine and the second component is an estimator with the adaptive system as input the estimated speed. The difference between the outputs of these flux estimators is used to correct the estimated speed [7].

Several MRAS structures are counted according to the choice of the variable *x*, such that the rotor fluxes, the electromotive force against or reactive power [8]. Compared to other approaches, the MRAS technique

improves the performance of the speed estimation that can be extended to very low speed [16].

For the double stator induction machine, the adaptive model is described by the current model [4], [8]:

$$\begin{cases} \dfrac{d\hat{\Phi}_{r\alpha i}}{dt} = \dfrac{L_m}{T_r}\left(i_{s\alpha 1} + i_{s\beta 1}\right) - \dfrac{1}{T_r}\hat{\Phi}_{r\alpha i} - \hat{\omega}_m\hat{\Phi}_{r\beta i} \\ \dfrac{d\hat{\Phi}_{r\beta i}}{dt} = \dfrac{L_m}{T_r}\left(i_{s\alpha 1} + i_{s\beta 1}\right) - \dfrac{1}{T_r}\hat{\Phi}_{r\beta i} + \hat{\omega}_m\hat{\Phi}_{r\alpha i} \end{cases} \quad (16)$$

The reference model is given by the voltage model [4, 8]:

$$\begin{cases} \dfrac{d\hat{\Phi}_{r\alpha v}}{dt} = \dfrac{L_r + L_m}{L_m}\left[V_{s\alpha 1} - R_s i_{s\alpha 1} - \sigma(L_s + L_m)\dfrac{di_{s\alpha 1}}{dt} - \dfrac{L_m L_r}{L_m + L_r}\dfrac{di_{s\alpha 2}}{dt}\right] \\ \dfrac{d\hat{\Phi}_{r\beta v}}{dt} = \dfrac{L_r + L_m}{L_m}\left[V_{s\beta 1} - R_s i_{s\beta 1} - \sigma(L_s + L_m)\dfrac{di_{s\beta 1}}{dt} - \dfrac{L_m L_r}{L_m + L_r}\dfrac{di_{s\beta 2}}{dt}\right] \end{cases} \quad (17)$$

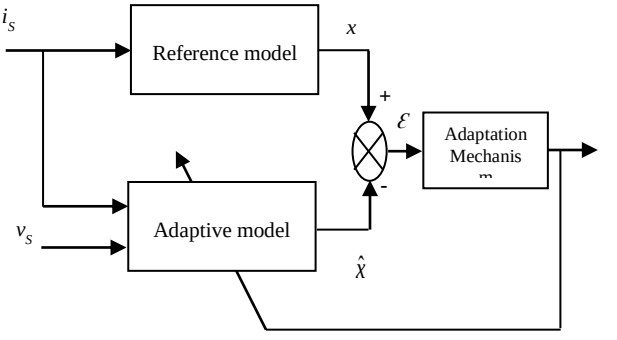

Fig.3. The overall structure of MRAS technique.

The flux error is calculated using the cross product [8], [16]:

$$\varepsilon = \hat{\Phi}_{r\alpha i}\hat{\Phi}_{r\beta v} - \hat{\Phi}_{r\alpha v}\hat{\Phi}_{r\beta i} \quad (18)$$

The adaptation law is classically given by a PI controller of the following expression [8], [16]:

$$\hat{\omega}_m = \varepsilon\left(k_p + \frac{k_i}{s}\right) \quad (19)$$

The block diagram of figure.4, illustrates the MRAS technique used for sensorless vector control of double stator induction motor.

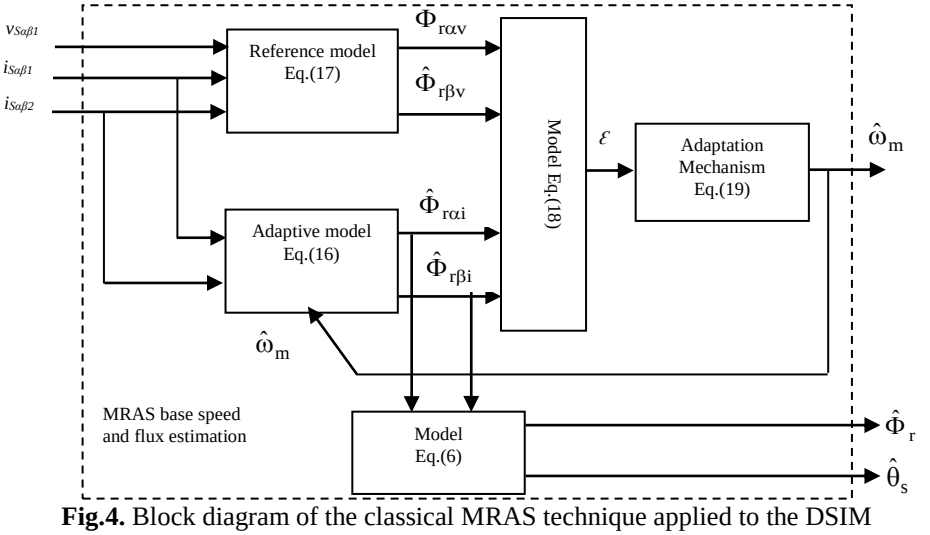

Fig.4. Block diagram of the classical MRAS technique applied to the DSIM

The use of classic PI regulator for this estimation method has not yielded satisfactory results regarding the rotor flux orientation and the imposed robustness test. Therefore, it's necessary to introduce more powerful regulators, which are based on a sliding-mode technique.

6. SLIDING MODE CONTROL THEORY

6.1. Multivariable System

The design of this control method can be divided into three stages:

a) Choice of sliding surfaces

J.J. Slotine proposes a general form of equation to determine the sliding surface which ensures the convergence of a variable to its desired value [11]:

$$S(x,t)=\left(\frac{d}{dt}+\lambda_x\right)^{r-1} e_x(t) \quad (20)$$

Where:

$e_x(t)$ The error in the output state;

$e_x(t)=x_{ref}(t)-x(t)$

λ_x Positive constant vector that interprets the desired control bandwidth.

r Relative degree, equal to the number of times it drives the output to the command.

b) Establishment of convergence conditions

The convergence conditions allow the dynamics of the system to converge towards the sliding surfaces. We retain from the literature to the following Lyapunov function:

$$V(x,t)=\frac{1}{2}S^2(x,t) \quad (21)$$

its derivative is:

$$\dot{V}(x,t)=S(x,t).\dot{S}(x,t) \quad (22)$$

So that the Lyapunov function decreases, it is sufficient to ensure that its derivative is negative. This is checked if:

$$S(x,t).\dot{S}(x,t)<0 \quad (23)$$

c) Control design

It is consist to find the expression of the equivalent control and the attractive control:

$$U(t)=U_{eq}(t)+U_n \quad (24)$$

The equivalent control $U_{eq}(t)$ is calculated on basis of the system behavior along the sliding mode surface, and the Lyapunov condition (23) gives the control U_n.

To check this condition and eliminate the chattering phenomenon [4], a simple solution is proposed for U_n:

$$U_n=-K\ \mathrm{Smooth}(S(x,t)) \quad (25)$$

The smooth function is given by:

$$\mathrm{Smooth}(S(x,t))=\frac{S(x,t)}{|S(x,t)|+\zeta} \quad (26)$$

Where:

K is the control gain.

ζ is a small positive parameter.

6.2. Sliding Mode Control Application

a) Speed sliding mode surface

The speed regulating surface whose relative degree r = 1 is of the following form:

$$S(\omega_m)=\omega_m^*-\omega_m+k\int(\omega_m^*-\omega_m)dt \quad (27)$$

By deriving the surface $S(\omega_r)$, we obtain:

$$\dot{S}(\omega_m)=\dot{\omega}_m^*-\dot{\omega}_m+k(\omega_m^*-\omega_m) \quad (28)$$

The mechanical equation gives:

$$\frac{d\omega_m}{dt}=\frac{1}{J}\left[p^2\frac{L_m}{L_m+L_r}(i_{sq1}+i_{sq2})\Phi_r^*-pT_L-k_f\omega_m\right] \quad (29)$$

Where: $\omega_m=p\Omega_m$

By posing $i_{sq1}+i_{sq2}=\tilde{i}_{sq}$ and substituting equation (29) into (28), we have:

$$\dot{S}(\omega_m)=\dot{\omega}_m^*+\frac{p}{J}T_L+\frac{k_f}{J}\omega_m+ +k(\omega_m^*-\omega_m)-\frac{p^2}{J}\frac{L_m}{L_m+L_r}\Phi_r^*\tilde{i}_{sq} \quad (30)$$

By letting:

$$f_1=\dot{\omega}_m^*+\frac{p}{J}T_L+\frac{k_f}{J}\omega_m$$

$$f_2=\frac{p^2}{J}\frac{L_m}{L_m+L_r}\Phi_r^*$$

Replacing the current $\tilde{i}_{sq}$ with the control current $\tilde{i}_{sq}=\tilde{i}_{sq(eq)}+\tilde{i}_{sq(n)}$ in equation (30), we find:

$$\dot{S}(\omega_m)=f_1+k(\omega_m^*-\omega_m)-f_2\tilde{i}_{sq(eq)}-f_2\tilde{i}_{sq(n)} \quad (31)$$

During sliding mode and in the established regime, we have $S(\omega_m)=0$ and therefore $\dot{S}(\omega_m)=0$ and $\tilde{i}_{sq(n)}=0$, hence we drive the formula of the equivalent control $\tilde{i}_{sq(eq)}$ from equation (31):

$$\tilde{i}_{sq(eq)}=\frac{f_1+k(\omega_m^*-\omega_m)}{f_2} \quad (32)$$

During the convergence mode, the Lyapunov condition (23) must be checked. By replacing (32) in (31), we obtain:

$$\dot{S}(\omega_m) = -f_2 \tilde{i}_{sq(n)} \quad (33)$$

We take for the attractive control:

$$\tilde{i}_{sq(n)} = K_{\omega_r} \frac{S(\omega_m)}{|S(\omega_m)| + \zeta_m} \quad (34)$$

b) Rotor flux sliding mode surface

Taking the same surface as that of the speed:

$$\dot{S}(\Phi_r) = \dot{\Phi}_r^* - \dot{\Phi}_r + k(\Phi_r^* - \Phi_r) \quad (35)$$

By posing $i_{sd1} + i_{sd2} = \tilde{i}_{sd}$ and substituting equation of rotor flux (9) in (35), we find:

$$\dot{S}(\Phi_r) = \dot{\Phi}_r^* - \frac{R_r}{L_m + L_r}\Phi_r - \frac{L_m R_r}{L_m + L_r}\tilde{i}_{sd} + k(\Phi_r^* - \Phi_r) \quad (36)$$

By letting:

$$f_1 = \dot{\Phi}_r^* - \frac{R_r}{L_m + L_r}\Phi_r$$

$$f_2 = \frac{L_m R_r}{L_m + L_r}$$

Replacing the current $\tilde{i}_{sd}$ with the control current $\tilde{i}_{sd} = \tilde{i}_{sd(eq)} + \tilde{i}_{sd(n)}$ in equation (36), we find:

$$\dot{S}(\Phi_r) = f_1 + k(\Phi_r^* - \Phi_r) - f_2 \tilde{i}_{sd(eq)} - f_2 \tilde{i}_{sd(n)} \quad (37)$$

During sliding mode and in the established regime, we have $S(\Phi_r) = 0$ and therefore $\dot{S}(\Phi_r) = 0$ and $\tilde{i}_{sd(n)} = 0$, hence we drive $\tilde{i}_{sd(eq)}$ from equation (37):

$$\tilde{i}_{sd(eq)} = \frac{f_1 + k(\Phi_r^* - \Phi_r)}{f_2} \quad (38)$$

During the convergence mode, the condition (23) must be checked. By substituting equation (38) into (37), we obtain:

$$\dot{S}(\Phi_r) = -f_2 \tilde{i}_{sd(n)} \quad (39)$$

We take for the attractive control:

$$\tilde{i}_{sd(n)} = K_{\Phi_r} \frac{S(\Phi_r)}{|S(\Phi_r)| + \zeta_{\Phi_r}} \quad (40)$$

c) Estimated speed sliding mode surface

The sliding surface of the estimated speed is:

$$S(\varepsilon) = \varepsilon + K\int \varepsilon.dt \quad (41)$$

Where: $K > 0$ and $\varepsilon = \Phi_{r\alpha i}\hat{\Phi}_{r\beta v} - \hat{\Phi}_{r\alpha v}\hat{\Phi}_{r\beta i}$

The derivative of $S(\varepsilon)$ gives

:

$$\dot{S}(\varepsilon) = \dot{\varepsilon} + K\varepsilon \quad (42)$$

Where:

$$\dot{\varepsilon} = \dot{\Phi}_{r\beta v}\Phi_{r\alpha i} + \dot{\Phi}_{r\alpha i}\Phi_{r\beta v} - \dot{\Phi}_{r\alpha v}\Phi_{r\beta i} - \dot{\Phi}_{r\beta i}\Phi_{r\alpha v} \quad (43)$$

The Substituting of the adaptive model equation (16) into (43) yields:

$$\dot{\varepsilon} = \dot{\Phi}_{r\beta v}\Phi_{r\alpha i} - \dot{\Phi}_{r\alpha v}\Phi_{r\beta i} + \frac{L_m}{T_r}\left(i_{s\alpha 1} + i_{s\beta 1}\right)\left(\Phi_{r\beta v} - \Phi_{r\alpha v}\right) - \frac{1}{T_r}\left(\Phi_{r\beta v}\hat{\Phi}_{r\alpha i} + \Phi_{r\alpha v}\hat{\Phi}_{r\beta i}\right) - \hat{\omega}_m\left(\Phi_{r\beta v}\hat{\Phi}_{r\beta i} + \Phi_{r\alpha v}\hat{\Phi}_{r\alpha i}\right) \quad (44)$$

By letting:

$$f_1 = \dot{\Phi}_{r\beta v}\Phi_{r\alpha i} - \dot{\Phi}_{r\alpha v}\Phi_{r\beta i} + \frac{L_m}{T_r}\left(i_{s\alpha 1} + i_{s\beta 1}\right)\left(\Phi_{r\beta v} - \Phi_{r\alpha v}\right) - \frac{1}{T_r}\left(\Phi_{r\beta v}\hat{\Phi}_{r\alpha i} + \Phi_{r\alpha v}\hat{\Phi}_{r\beta i}\right) \quad (45)$$

$$f_2 = \Phi_{r\beta v}\hat{\Phi}_{r\beta i} + \Phi_{r\alpha v}\hat{\Phi}_{r\alpha i} \quad (46)$$

Equations (42) and (44) can be written as:

$$\dot{\varepsilon} = f_1 - \hat{\omega}_m f_2 \quad (47)$$

And

$$\dot{S}(\varepsilon) = f_1 - \hat{\omega}_m f_2 + K\varepsilon \quad (48)$$

By replacing $\hat{\omega}_m$ with equivalent and attractive control $\hat{\omega}_m = \hat{\omega}_{m(eq)} + \hat{\omega}_{m(n)}$ in equation (48), we find:

$$\dot{S}(\varepsilon) = f_1 - \hat{\omega}_{m(eq)} f_2 + \hat{\omega}_{m(n)} f_2 + K\varepsilon \quad (49)$$

During sliding mode and in the established regime, we have $S(\varepsilon)=0$ and therefore $\dot{S}(\varepsilon)=0$ and $\hat{\omega}_{m(n)}=0$, hence:

$$\hat{\omega}_{m(eq)}=\frac{f_1+K\varepsilon}{f_2} \quad (50)$$

During the convergence mode, the Lyapunov condition (23) must be checked. By replacing (50) into (49), we obtain:

$$\dot{S}(\varepsilon)=f_2\hat{\omega}_{m(n)} \quad (51)$$

We take for the attractive control:

$$\hat{\omega}_{m(n)}=K_\varepsilon\frac{S(\varepsilon)}{|S(\varepsilon)|+\zeta_\varepsilon} \quad (52)$$

the block diagram of the sliding-mode MRAS estimator applied to the DSIM is shown in Fig. 5.

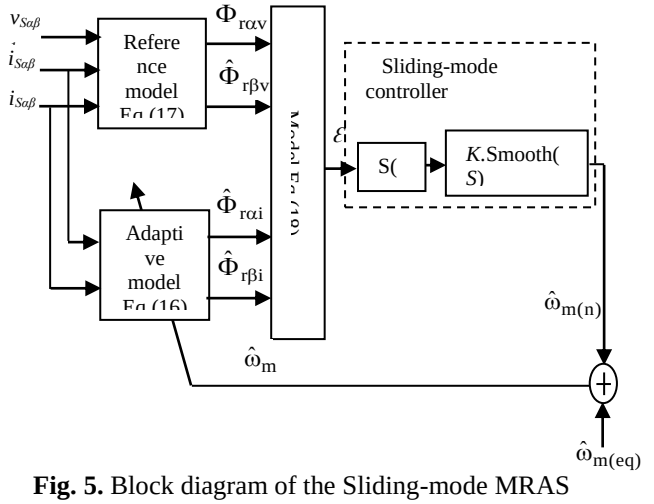

Fig. 5. Block diagram of the Sliding-mode MRAS technique applied to the DSIM.

7. SIMULATION RESULTS

Using the block diagram of Fig. 1, the simulation was carried out under the same conditions as the conventional control with the following adjustment parameters (Tab.1)

To validate the static and the dynamic performances of the sliding-mode MRAS speed estimator (Fig. 6), different simulation scenarios are considered.

The speed trajectory up to the nominal value +280rd /sec and returns to -280rd /sec according to different profiles. For this speed step, a load disturbance of 14 N.m is applied between 1.5sec and 2.5sec with a reversal of speed rotation at t = 3.5s.

Table 1. Sliding surfaces setting parameters

Parameter	$S(\omega_m)$	$S(\Phi_r)$	$S(\varepsilon_{\hat{\omega}_m})$
K	100	120	130
ζ	0.4	0.01	0.1

8. DISCUSSION

Figure.6 illustrates the electromagnetic torque, stator phase current, real and estimated rotor flux, real and estimated speed and corresponding estimation errors of a sliding-mode MRAS speed sensorless direct vector control of DSIM. As shown in this figure, the sliding-mode estimator has good speed and flux tracking with a dynamic error is not important and a static error is practically zero.

8.1. Robustness Test

We perform a robustness test with respect to the variation of the different parameters separately; rotor resistance, stator resistors, mutual inductance and inertia.

In this simulation, the DSIM runs with the speeds 150rd/sec and 30rd/sec considering increasing of the parameters. At start-up the DSIM operates with the nominal values of these parameters, and between the time t = 1.5sec and 2.5sec, a step of +50% of each parameter is applied separately.

Figure (7) shows the speed and the rotor flux responses for a +50% increase in the rotor resistance. We observe that the speed increases (overshoot of 0.66% of its value) compared to the nominal parameters. At low speed (Figure 8), the speed is also affected, but the decoupling is maintained.

Figure (9) shows that the speed is not affected by a +50% increase in the stator resistance, but at low speed (Figure 10) the speed response is oscillatory and the control almost lost.

In the figures (11) and (12), the speed and rotor flux are shown when the mutual inductance increases by + 50% of its nominal value. We see in these figures, that the variation of the mutual inductance has a remarkable influence on the speed and especially on the quality of the rotor flux orientation.

Through the figures (13) and (14), we find that a +100% increase in the inertia has little effect on the control performance for high speed or low speed. Indeed, we see a slight increase in the speed response time with a small overshoot at startup and at the speed reversion. However, the rotor flux is perfectly oriented.

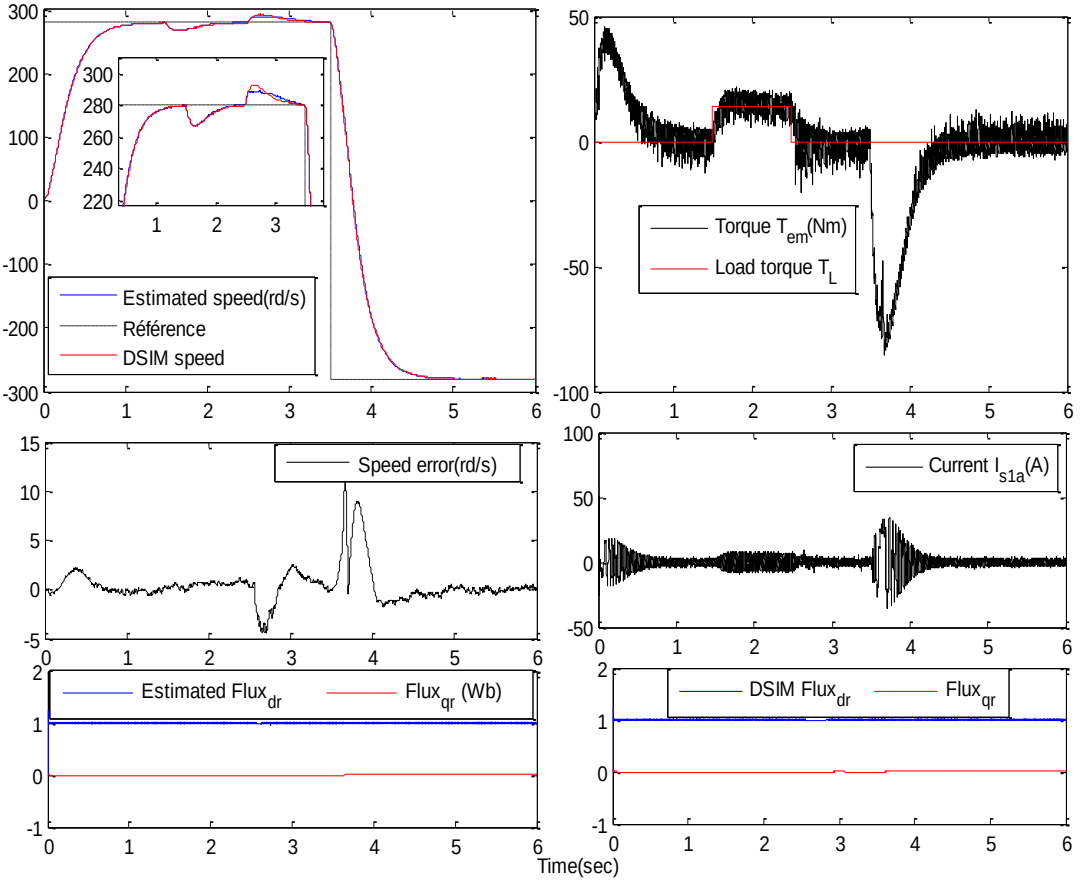

Fig. 6. Simulation results for sliding-mode MRAS speed sensorless vector control of DSIM.

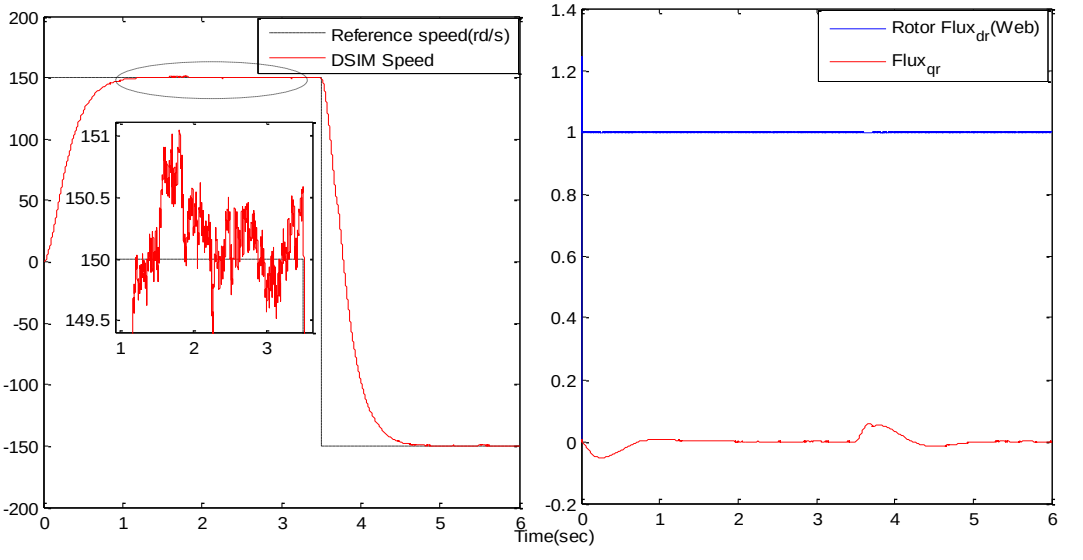

Fig. 7. Robustness test: for parameter variation of +50%Rr; speed and rotor flux results.

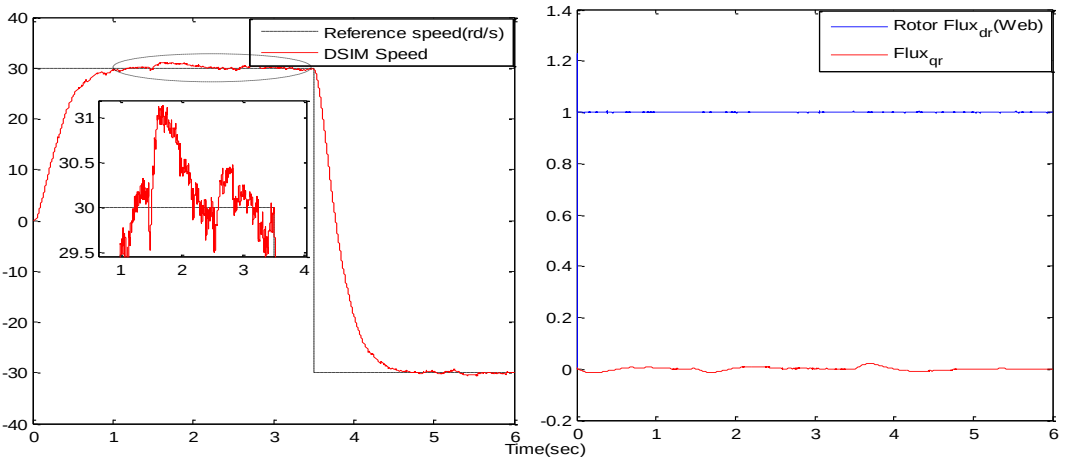

Fig. 8. Robustness test: for parameter variation of +50%Rr in low speed.

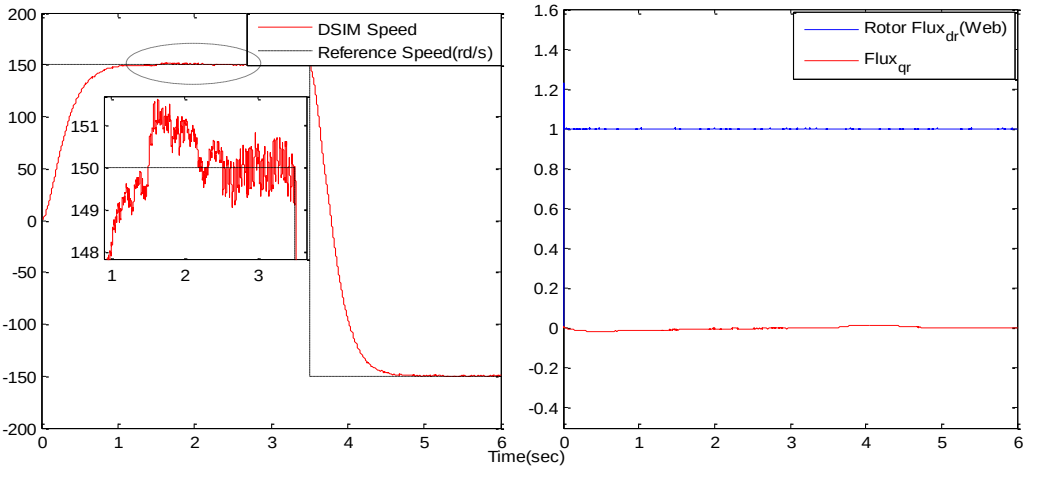

Fig. 9. Robustness test: for parameter variation of +50%$R_{s1,2}$; speed and rotor flux results.

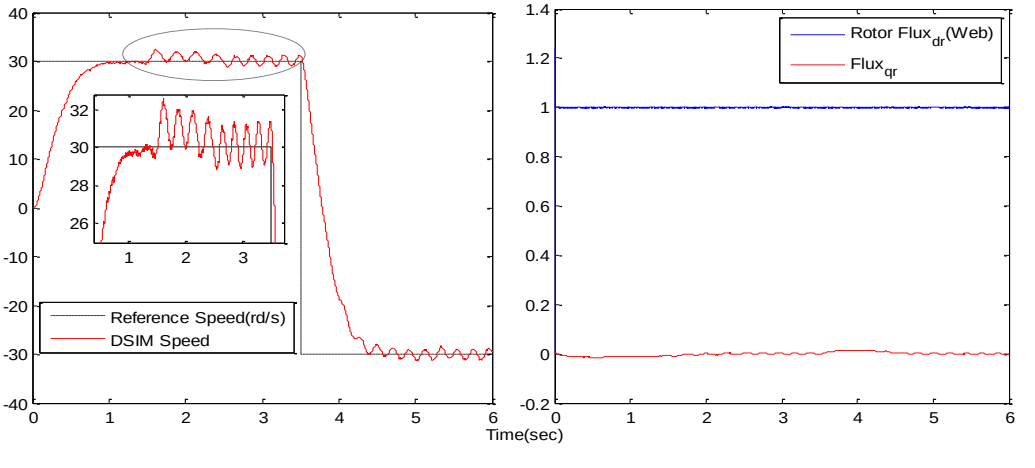

Fig. 10. Robustness test: for parameter variation of +50%$R_{s1,2}$ in low speed.

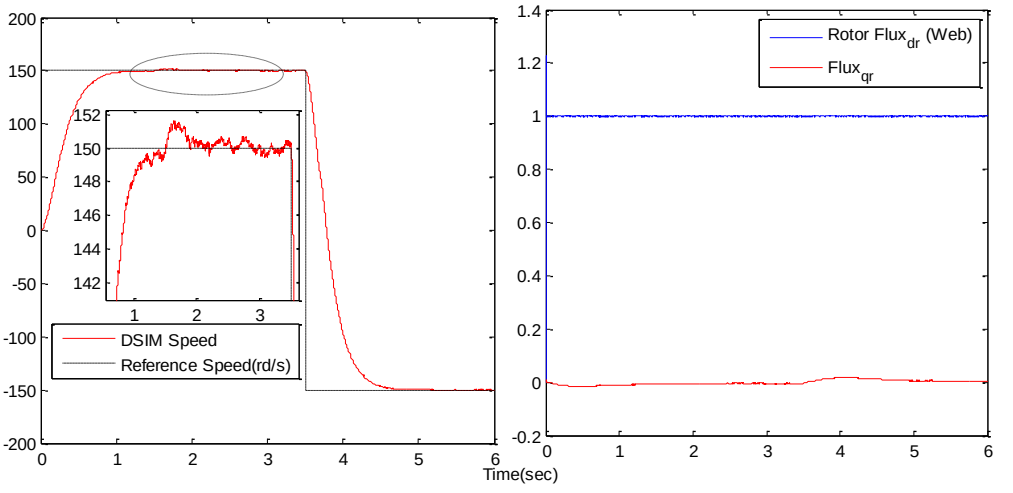

Fig. 11. Robustness test: for parameter variation of -50%Lm; speed and rotor flux results.

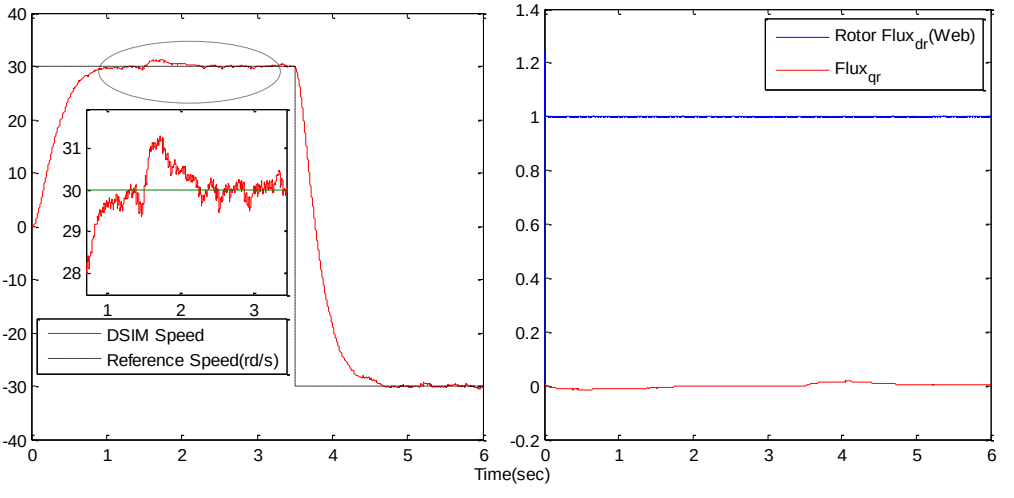

Fig. 12. Robustness test: for parameter variation of -50%Lm in low speed.

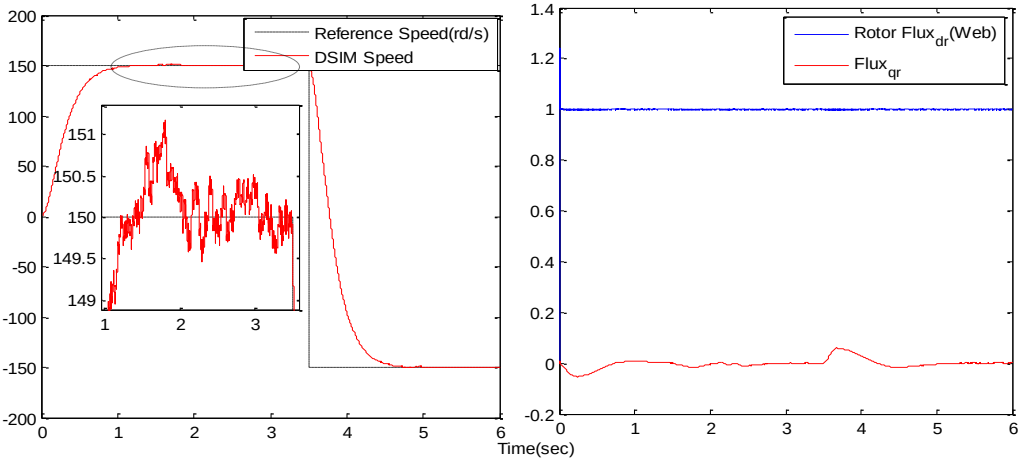

Fig. 13. Robustness test: for parameter variation of +100%J; speed and rotor flux results.

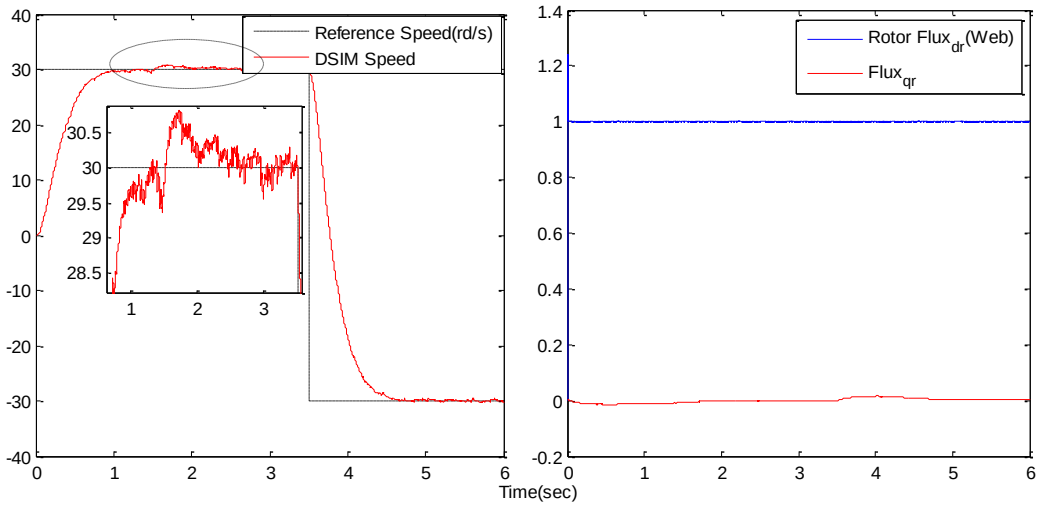

Fig. 14. Robustness test: for parameter variation of +100%J in low speed.

9. CONCLUSION

In this paper we are presented the sliding-mode MRAS estimator for speed sensorless vector control of a DSIM.

The sensorless speed operation increases reliability, reduces the complexity and the cost of the system. Indeed, the speed variation of the double stator induction motor in the low-speed range is a difficult problem to be overcome with respect to the parametric variation and in particular the stators resistances and the mutual inductance, thus causing the instability of the system.

From the obtained results, it can be concluded that the studied estimation techniques are valid for the nominal conditions, even satisfying the operations in variable speed drive and even when the motor is loaded, on the other hand they have a good robustness to the parameters variation, thus achieving good static and dynamic performance.

10. APPENDIX

Double stator induction motor parameters [4], [12], [13]

P_n=4.5kW, f=50Hz, $V_{n(\Delta/Y)}$=220/380V, $I_{n(\Delta/Y)}$=6.5A, Ω_n=2751rpm, p=1

R_{s1}= R_{s2}=3.72Ω, R_r =2.12Ω, L_{s1}= L_{s2}= 0.022H, L_r = 0.006H, L_m =0.3672H

J =0.0625 Kgm^2, K_f =0.001 Nm(rad/s)$^{-1}$

REFERENCES

[1] P.Vas. "**Sensorless Vector and Direct Torque Control**", *Oxford University Press*, Oxford, 1998.

[2] M. Menaa, O. Touhami, R. Ibtiouen, M. Fadel, "**Sensorless Direct Vector Control of An Induction Motor**". *Control Engineering Practice*, 2008, Vol. 16, pp.67-77.

[3] R. Kianinezhad, B. Nahid-Mobarakeh, F. Betin, G.A. Capolino, "**Sensorless Field-Oriented Control for Six Phase Induction Machines**". *IEEE Trans. on Ind*. Appl, 2005, Vol. 71, pp. 999-1006.

[4] H. Khouidmi, A. Massoum, "**Reduced-order Sliding Mode Observer Based Speed Sensorless Vector Control of Double Stator Induction Motor**", *Journal of Applied Sciences, Acta Polytechnica Hungarica*, 2014, Vol. 11, (06), pp. 229-249.

[5] R. Nilsen, M.P. Kazmierkowski, "**Reduced-Order Observer with Parameter Adaptation for Fast Rotor Flux Estimation in Induction Machine**". *IEE Proceedings*, 1989, Vol. 136(1), pp. 35-43.

[6] K. Marouani, K. Chakou, F. Khoucha, B. Tabache, and A. Kheloui, "**Observation and Measurement of Magnetic Flux in a Dual Star Induction Machine**", *19th Mediterranean Conference on Control and Automation Aquis Corfu Holiday Palace*, Corfu, Greece June 20-23, pp. 289-294, 2011.

[7] M. Rizwan Khan, I. Atif, A. Mukhtar, "**MRAS-based Sensorless Control of a Vector Controlled Five-Phase Induction Motor Drive**". *Electric Power Systems Research*, 2008, Vol. 78, pp. 1311–1321.

[8] DJ. Cherifi, Y. Miloud and A. Tahri, "**Performance Evaluation Of A Sensorless Induction Motor Drive Using A MRAS Speed Observer**", *Journal of Current Research in Science*, 2013, Vol. 1, No. 2, pp. 71-78.

[9] K. Kouzi, T. Seghier and A. Natouri, "**Fuzzy Speed Sensorless Vector Control of Dual Star Induction Motor Drive Using MRAS Approach**", *International Journal of Electronics and Electrical Engineering*, 2015, Vol. 3, No. 6, pp. 445-450.

[10] A. F. Filippov, "**Differential Equations with Discontinuous Right-Hand Side**", *Matematicheski Sbornik*, Vol. 51, No. 01, pp. 99–128, 1960.

[11] J. J. Slotine, J. K. Hedrick, E. A. Mizawa, "**On Sliding Observer for Nonlinear Systems**", *J.*

Dynam. Syst. Measur. Contr., Vol. 01, pp. 239/245, 1985.

[12] H. Khouidmi, A. Massoum and A. Meroufel, "**Dual Star Induction Motor Drive: Modelling, Supplying and Control**", *International Journal of Electrical and Power Engineering*, 2011, Vol. 05, pp. 28-34.

[13] R. Sadouni, A. Meroufel, "**Indirect Rotor Field-oriented Control (IRFOC) of a Dual Star Induction Machine (DSIM) Using a Fuzzy Controller**", *Journal of Applied Sciences, Acta Polytechnica Hungarica*, 2012, Vol. 9, (04), pp. 177-192.

[14] B. Ghalem, A. Bendiabdellah, "**Six-Phase Matrix Converter Fed Double Star Induction Motor**", *Journal of Applied Sciences, Acta Polytechnica Hungarica*, 2010, Vol. 7, No. (03), pp. 163-176.

[15] F. Blaschke, "**The Principle Of Field Orientation Applied To The New Trans-Vector Closed-Loop Control System for Rotating Field Machines**", *Siemens-Review*, Vol. 39, pp. 217-220, 1972.

[16] C. Shauder, "**Adaptive Speed Identification For Vector Control of Induction Motors Without Rotational Transducers**", *IEEE Transations on Industry Applications* 1992, 28:1054-1061.